Reduced pathology and improved behavioral performance in Alzheimer's disease mice vaccinated with HSV amplicons expressing amyloid-beta and interleukin-4

Maria E. Frazer[3], **Jennifer E. Hughes**[3], **Michael A. Mastrangelo**[3], **Jennifer L. Tibbens**[3], **Howard J. Federoff**[1,2,3,4], and **William J. Bowers**[1,2,3,*]

[1]*Department of Neurology, University of Rochester School of Medicine and Dentistry, Rochester, NY 14642*

[2]*Department of Microbiology and Immunology, University of Rochester School of Medicine and Dentistry, Rochester, NY 14642*

[3]*Center for Aging and Developmental Biology, University of Rochester School of Medicine and Dentistry, Rochester, NY 14642*

Abstract

Immunotherapeutics designed to dissolve existing amyloid plaques or to interrupt amyloid-beta (Aβ) accumulation may be feasible for treatment and/or prevention of Alzheimer's disease (AD). "Shaping" immune responses elicited against Aβ is requisite to generate an efficacious and safe outcome by minimizing the possibility of deleterious inflammatory reactions in the brain as observed in clinical testing of Aβ peptide/adjuvant-based modalities. Herpes Simplex Virus (HSV)-based amplicons can co-express multiple antigens and/or immunomodulatory genes due to their large genetic size capacity, thereby facilitating antigen-specific immune response shaping. We have constructed an amplicon ($HSV_{IE}Aβ_{CMV}IL$-4) that co-delivers $Aβ_{1-42}$ with interleukin-4, a cytokine that promotes the generation of Th2-like T cell responses, which are favored in the setting of AD immunotherapy. Triple-transgenic AD (3xTg-AD) mice, which progressively develop both amyloid and neurofibrillary tangle pathology, were vaccinated thrice with $HSV_{IE}Aβ_{CMV}IL$-4, or a set of control amplicon vectors. Increased Th2-related, Aβ-specific antibodies, improved learning and memory functioning, and prevention of AD-related amyloid and tau pathological progression were observed in $HSV_{IE}Aβ_{CMV}IL$-4 vaccinated mice as compared to the other experimental groups. Our study underscores the potential of Aβ immunotherapy for AD and highlights the potency of amplicons to facilitate immune response modulation to a disease-relevant antigen.

Keywords

Alzheimer's disease; behavior; Barnes maze; Aβ deposition; Tau; triple-transgenic mice

Introduction

Alzheimer's disease (AD) is a progressive neurodegenerative disorder commonly associated with dementia and a decline in performance of normal age-related activities. As the disease progresses, cognitive decline in episodic and semantic memory, as well as decision-making,

[*]Corresponding Author, William J. Bowers, Ph.D., Department of Neurology, Center for Aging and Developmental Biology, University of Rochester School of Medicine and Dentistry, 601 Elmwood Ave., Box 645, Rochester, NY 14642 USA, Phone: 585-273-2195, Fax: 585-276-1947, E-mail address: william_bowers@urmc.rochester.edu
[4]Present Address: Office of the Executive Vice President for Health Sciences, Georgetown University Medical Center, Washington, DC

judgment, language and spatial orientation become profoundly evident (reviewed by [1]). Hallmark features of AD pathology include, but are not limited to, extracellular plaques of the peptide amyloid beta (Aβ) and hyperphosphorylation of tau protein, presenting as intraneuronal neurofibrillary tangles (NFTs), that proceeds in a spatial and temporal pattern with diminishing synaptic density and eventually leads to marked neuronal loss [2,3].

The societal burden imparted by this debilitating disease presages the derivation and testing of new natural history modifying therapeutic approaches. Presently available therapeutic agents employed to treat AD are designed to manage cognitive and emotional symptoms of the disease (reviewed by [4]). These interventions provide only transient symptomatic benefit, as they are not designed to specifically target pathologic mechanisms underlying the genesis of AD. The amyloid cascade hypothesis suggests modalities, which will abrogate the proteolytic generation of Aβ peptides, prevent Aβ fibrillogenesis, and/or amyloid deposition would impact the onset and/or severity of AD [5].

A promising, yet inherently complex, means of inhibiting Aβ fibrillogenesis and/or deposition relates to the use of the host immune system to mount specific immune responses against the self-peptide, Aβ. The findings from a variety of immune-based strategies speak to the promise of this approach [6-10], but also reveal the potential for morbid complications of AD immunotherapy [11-13]. Given these mixed clinical results, Aβ-directed immunotherapy warrants further study particularly if an optimal immune response/antibody can be developed. Helper T cell function, normally required for an effective antibody response, is believed to exclusively require Th2-biased responses in the setting of AD immunotherapy, as a strong Th1 response carries the risk of inducing a local inflammatory response to the APP antigen should Aβ-primed T cells penetrate the blood/brain barrier. Although presently untested in human clinical trials, gene-based vaccination technology due to its inherent versatility may allow for greater precision in antigen presentation and immunomodulation that could lead to safer and more efficacious vaccines for AD [14,15].

Given its ease of manipulation, absence of immunosuppressive viral genes, ability to efficiently transduce antigen presenting cells, and large transgene capacity, the Herpes simplex virus (HSV) amplicon represents a well-positioned platform on which to build an Aβ-directed AD vaccine [16-19]. Our laboratory has previously employed amplicons to elicit distinctive immune responses against Aβ using a fused molecular adjuvant approach [15]. Herein, we describe the derivation of an Aβ-expressing amplicon vaccine (HSV$_{IE}$Aβ$_{CMV}$IL-4) that co-delivers interleukin-4, a cytokine expressed by Th2 T cells and demonstrated to promote Th2-biased immune responses [20]. HSV$_{IE}$Aβ$_{CMV}$IL-4-mediated vaccination of triple-transgenic AD (3xTg-AD) mice [21,22], which develop both amyloid deposition and tau-related dysfunction that mirrors the spatial and temporal progression of pathology observed in human AD, resulted in suppression of AD-related pathological hallmark appearance and concomitant improvement in learning and memory functioning.

Results

Three HSV amplicon vectors were constructed (Fig. 1a): pHSV$_{IE}$1$_{CMV}$2 served as a no-insert control and harbored only the HSV origin of replication and packaging signal along with empty HSV immediate-early 4/5 (IE4/5) gene promoter and cytomegalovirus (CMV) immediate-early promoter-driven transcription cassettes; pHSV$_{IE}$Aβ$_{CMV}$2 contained the DNA sequence for human Aβ$_{1-42}$ peptide under the transcriptional control of the HSV IE4/5 gene promoter; and pHSV$_{IE}$Aβ$_{CMV}$IL-4 harbored Aβ$_{1-42}$ downstream of the HSV IE4/5 gene promoter and murine interleukin-4 under the transcriptional control of the CMV promoter. Testing of pHSV$_{IE}$Aβ$_{CMV}$IL-4 *in vitro* by transfection of baby hamster kidney (BHK) cells and ELISA analysis of cell culture supernatants demonstrated that this amplicon expressed high levels of

secreted murine IL-4 (Fig. 1b). The integrity of the $A\beta_{1-42}$ expression cassette was confirmed previously [15]. The amplicon plasmids were subsequently packaged into helper virus-free virus stocks and titered using previously described methodologies [23,24].

Two month-old male 3xTg-AD mice each received three injections of 1×10^6 transduction units of a designated amplicon vaccine. The timing of vaccinations, blood draws, behavioral assessments by Barnes maze, and immunohistochemical analyses are depicted schematically in Fig. 1c. For these experiments, we chose to allow primed mice to "rest" for 120 d before the final boost. Since HSV-1 amplicon vectors induce high and transient levels of transgene (antigen) expression [25], we predicted that the overwhelming majority of $A\beta$-specific T and B cells present at the time of the final boost would consist of memory immune cells (reviewed by [26]).

$HSV_{IE}A\beta_{CMV}$IL-4 vaccinated 3xTg-AD mice exhibit enhanced levels of $A\beta_{1-42}$ specific antibodies that exhibit Th2 bias

After the first and second set of immunizations, mice receiving $HSV_{IE}A\beta_{CMV}2$, $HSV_{IE}A\beta_{CMV}$IL-4, or $HSV_{IE}1_{CMV}2$ exhibited no significant differences in anti-$A\beta$ antibody levels (Fig. 2a). Following the final immunization, however, $HSV_{IE}A\beta_{CMV}$IL-4 vaccinated mice harbored significantly higher levels of circulating $A\beta$-specific antibodies than 3xTg-AD mice receiving either $HSV_{IE}A\beta_{CMV}2$ or the empty vector control $HSV_{IE}1_{CMV}2$ amplicon, indicating that co-delivery of IL-4 during amplicon vaccination augmented the overall $A\beta$-directed humoral response (Fig. 2a). The delivery of $HSV_{IE}A\beta_{CMV}2$ amplicon was surprisingly unable to break tolerance in 3xTg-AD mice, as levels of α-$A\beta$ antibodies did not increase over those found in mice vaccinated with the $HSV_{IE}1_{CMV}2$ control vector. It is also of note that $HSV_{IE}1_{CMV}2$-vaccinated mice did exhibit detectable anti-$A\beta$ antibodies. This is not surprising since the age-related development of anti-$A\beta$ antibodies in non-vaccinated AD mice has been described previously [27]. Serum samples obtained at the 9-month time point were further examined to isotype the anti-$A\beta$ antibodies elaborated as a result of amplicon vaccination. Sera from $HSV_{IE}A\beta_{CMV}$IL-4-immunized 3xTg-AD mice possessed a higher representation of anti-$A\beta$ specific antibodies of the Th2-derived IgG1 isotype and suppressed levels of Th1-related IgG2b, IgG2c, and IgG3 isotypes, indicating that the co-expression of IL-4 led to a Th2-like immune response bias.

$HSV_{IE}A\beta_{CMV}$IL-4 vaccinated mice exhibit improved performance on the Barnes Maze

Long-term spatial memory, which is adversely affected in AD and is partially dependent upon hippocampal circuitry function, was assessed in 3xTg-AD mice using the Barnes maze spatial memory paradigm [28]. The mouse must learn and remember the relationship among distal spatial cues to navigate to the escape box. Mice were tested in the Barnes maze at 2 months of age to establish baseline data and at 6 and 11 months of age to gauge effects that amplicon-mediated vaccination may impart on the various output measures of the Barnes maze paradigm. The following measures were assessed: distance traveled by each mouse to reach the goal box, errors made during the search for the correct escape hole, and the time required by the mouse to enter the escape box (latency). If the $A\beta$-directed amplicon vaccines imparted the intended humoral response, we would expect to observe shorter distances traveled, fewer errors made, and shorter latency times. However, should amplicon-based $A\beta$ vaccination elicit deleterious immune responses, such adverse events may affect cognitive functioning, where $HSV_{IE}A\beta_{CMV}2$ and/or $HSV_{IE}A\beta_{CMV}$IL-4 injected mice perform less optimally as compared to $HSV_{IE}1_{CMV}2$ control amplicon-vaccinated mice.

Measurements of distance, errors, and latency amongst the amplicon-immunized groups were highly similar at the 2-month baseline time point and at the 6-month mid-point of the study, when AD-related pathologies are minimally detectable in 3xTg-AD mice (Fig. 3; [21,22]). At

the 11-month time point, just prior to sacrifice, $HSV_{IE}A\beta_{CMV}IL-4$ vaccinated mice exhibited improved performance in each of the Barnes maze parameters assessed. Briefly, $HSV_{IE}A\beta_{CMV}IL-4$ mice traveled less distance than $HSV_{IE}1_{CMV}2$ vaccinated mice (Fig. 3a; P<0.05), made fewer errors (Fig. 3b) and completed the maze with lower latency times (Fig. 3c) than $HSV_{IE}1_{CMV}2$ (P<0.05) and $HSV_{IE}A\beta_{CMV}2$ (P<0.05) vaccinated mice. In aggregate, these data indicate that $HSV_{IE}A\beta_{CMV}IL-4$ vaccination improved spatial learning and memory functioning in 3xTg-AD mice presumably via preventing Aβ accumulation in the brain and downstream consequences of Aβ toxicity. Moreover, it did not appear that Aβ-directed amplicon vaccination negatively impacted Barnes maze performance as $HSV_{IE}A\beta_{CMV}2$ injected mice performed similarly to $HSV_{IE}1_{CMV}2$ treated control mice in all parameters assessed.

Vaccination-mediated effects on severity of AD-related pathology

We assessed the extent to which amplicon vaccination led to prevention of AD-related pathologies by performing immunohistochemical analysis combined with quantitative image analysis on brain sections from immunized mice for human APP/Aβ, unphosphorylated human tau transgene product, pathologic tau phospho-epitope, astrogliosis, and microglial activation. Because the 3xTg-AD mouse displays differential severities of AD-related pathologies along the rostral to caudal axis, we analyzed the CA_1 of the hippocampus at two points (-1.28 and -2.12 mm from Bregma), which were designated as Areas I and II. We also analyzed the subiculum region lying more caudally (-2.75 mm from Bregma) as this brain region exhibits pronounced amyloid and tau pathology in 3xTg-AD mice [21,22], and designated it as Area III. The entorhinal cortex was also examined since it is also affected during AD pathogenesis and was designated Area IV.

Using the 6E10 antibody to detect human APP and Aβ species, we observed profound differences in staining amongst the cohorts of vaccinated mice. $HSV_{IE}A\beta_{CMV}2$ and $HSV_{IE}1_{CMV}2$ immunized mice exhibited appreciable APP/Aβ staining intensities that were nearly indistinguishable from non-vaccinated, age-matched control 3xTg-AD mice (NVC; Fig. 4). Conversely, $HSV_{IE}A\beta_{CMV}IL-4$ injected mice harbored no immunologically detectable APP/Aβ staining in any of the brain regions assessed and hence, exhibited a marked suppression in amyloid deposition as compared to the other vaccination groups (Fig. 4q). APP/Aβ staining in the entorhinal cortex (Area IV) was minimal at this time point and hence, differences in staining intensities amongst the vaccinated and NVC mice were not discernable. To demonstrate that the loss of 6E10 immunopositivity was not due to diminution in hAPP[swe] transgene expression, brain sections from a subset of $HSV_{IE}A\beta_{CMV}IL-4$ vaccinated mice were stained with a hAPP-specific antibody, Y188. These mice exhibited robust hAPP[swe] expression, indicating the loss of 6E10 immunopositivity in these mice is primarily due to the reduction in detectable Aβ peptides (Fig. 5).

The amyloid cascade hypothesis suggests that prevention of amyloid deposition would impact the onset and/or severity of downstream pathologies associated with AD, including tau hyperphosphorylation and dysfunction [5]. Immunohistochemical analysis of unphosphorylated human tau using the HT7 antibody revealed similar staining patterns and intensities in Areas caudal hippocampus and entorhinal cortex for all vaccinated and non-vaccinate animals (Areas II, and IV; Fig. 6). Of note, $HSV_{IE}A\beta_{CMV}IL-4$ vaccinated 3xTg-AD mice exhibited statistically higher intensities of unphosphorylated tau staining in the subiculum as compared to the other two vaccine groups and NVC group, suggesting potential effects on the expression and/or turnover of the human tau transgene product in neurons residing in this brain sub-region (Fig. 6q). Conversely, $HSV_{IE}A\beta_{CMV}IL-4$ vaccinated 3xTg-AD mice exhibited suppressed HT7 staining in rostral hippocampus. Moreover, the pattern of HT7 staining appeared more pyramidal neuron cell body-associated in hippocampal regions than

that of other groups where staining of neuronal processes was more evident. Strikingly, analysis of phosphorylated tau using the AT180 antibody, which recognizes tau phosphorylated at Ser-231 and Thr-235, showed that brains from $HSV_{IE}A\beta_{CMV}IL$-4 vaccinated animals harbored no detectable AT180 staining in Areas I, II, III, or IV (Fig. 7). Signal quantitation revealed statistically significant differences in Areas I, II, and III between the $HSV_{IE}A\beta_{CMV}IL$-4 group and each of the other cohorts. These data indicate that prevention of Aβ deposition via prophylactic amplicon-mediated co-delivery of Aβ_{1-42} and the Th2 cytokine, IL-4, delays or halts the age-dependent, pathogenic phosphorylation of tau in 3xTg-AD mice, thereby providing further support to the amyloid cascade hypothesis.

There exists the possibility that amplicon-mediated vaccination of 3xTg-AD mice led to the exacerbation of previously described neuroinflammatory conditions, including astrogliosis and microglial activation [29]. Glial fibrillary acidic protein (GFAP) immunohistochemistry for astrocytes and F4/80-directed immunohistochemical analysis of activated microglia in the brains of vaccinated mice did not reveal any qualitative alterations in staining patterns or intensities (Fig. 8). Moreover, hematoxylin and eosin staining of brain sections did not show evidence for overt immune cell infiltration (Supplementary Fig. 1), which in aggregate indicated that repeated peripheral administration of the HSV amplicon-based vaccines did not overtly enhance the neuroinflammatory state resident in the aging 3xTg-AD mouse brain.

Discussion

Previously explored Aβ-directed immunotherapies have been largely based upon conventional peptide and adjuvant vaccination platforms [6-8]. More recently, gene-based methodologies have been explored [14,15]. These prior immunization strategies were shown to retard the progression of disease-related pathology and improve pathologic, behavioral, and electrophysiological correlates in animal models of AD. However, the safety concerns raised in response to the manifestation of meningoencephalitis in a subset of Phase II clinical trial subjects implore the examination of vaccine strategies that offer stricter control over resultant Aβ-directed responses [12,30-32]. In the present study, we demonstrate that a prime-boost strategy involving an HSV amplicon vector co-delivering an Aβ_{1-42} immunogen and interleukin-4 results in an enhanced Aβ-directed immune response with Th2 bias in 3xTg-AD mice. These mice exhibited superior learning and memory performance as assessed by the Barnes maze and diminished AD-related amyloid and tau pathologies in their brains at 11 months of age.

Previously, we had demonstrated that an amplicon vector expressing Aβ_{1-42} alone or Aβ_{1-42} as an in-frame fusion with tetanus toxin Fragment C was able to engender detectable and differential Aβ-specific humoral responses in the amyloidogenic Tg2576 mouse AD model [15]. However, $HSV_{IE}A\beta_{CMV}2$ vaccination of 3xTg-AD mice did not exhibit anti-Aβ antibody levels that were higher than a cohort immunized with the $HSV_{IE}1_{CMV}2$ empty vector control amplicon (Fig. 2). This discrepancy could be due to the inherent levels of APP^{Swe} transgene product and ratios of proteolytically processed Aβ species that are expressed in each AD mouse model. The Tg2576 mouse expresses APP^{swe} under the transcriptional control of the hamster prion protein (PrP) promoter, while the 3xTg-AD mouse expresses APP^{Swe} and tau^{P301L} under control of the Thy1-2 promoter, which may account for the differential abilities of amplicon-mediated vaccination to break tolerance in the mouse models and suppress amyloid deposition [22,33]. Moreover, the presence of the PS1 knock-in mutation in the 3xTg-AD mouse results in the generation of even higher ratios of Aβ_{1-42} to Aβ_{1-40} peptide species than observed in the Tg2576 mouse [22]. It is of note that the antibody titers derived from our ampliocn-based vaccination paradigm, although sufficient to markedly alter AD-related pathologies, are rather modest compared to those elicited by other active anti-Aβ immunotherapies. One could posit that the "quality" of the humoral response (e.g., isotypes engendered, antibody avidity,

recognized Aβ epitopes, etc.) is an important predictor of a given AD vaccine's "efficacy". In fact, Sigurdsson and colleages showed previously that repeated vaccination of Tg2476 mice with shorter Aβ derivatives led to lower overall IgG titers, but these vaccines led to enhanced Aβ clearance and behavioral maze performance. The authors attributed these results to an enhanced IgM antibody component that acted as an Aβ sync at the blood-brain barrier to efficiently remove Aβ peptide from the brain compartment [34]. Hence, vaccination may require an approach that produces the optimal combination of anti-Aβ humoral responses, which co-expression of $A\beta_{1-42}$ peptide with the Th2 cytokine, IL-4, provided in the present study.

$HSV_{IE}A\beta_{CMV}IL$-4 immunized mice exhibited virtually no Aβ burden (6E10 immunohistochemistry) that paralleled a reduction in levels of hyperphosphorylated tau (AT180), strongly supporting the purported link between Aβ and tau dysfunction as outlined in the amyloid cascade hypothesis. Oddo and colleagues previously observed that transient diminution of Aβ with cerebrally infused anti-Aβ antibody led to transient prevention of tau hyperphosphorylation in 3xTg-AD mice [35]. This tau effect required that Aβ clearance occur prior to appearance of initial tau hyperphosphorylation in these mice, similar in concept to our prophylactic vaccine approach. Such results suggest that patients with early-stage disease represent more ideal candidates for immune-based interventions targeting pathogenic Aβ peptides.

Developing an immunotherapeutic approach for AD is a challenging endeavor given the extant inflammatory state within the AD brain. Our analysis of amplicon-based Aβ vaccination in the 3xTg-AD mouse model did not show evidence of overt exacerbation of microglial and astrocytic activation (Fig. 7). Previously, however, we observed that Tg2576 mice immunized with an $A\beta_{1-42}$-expressing amplicon led to a marked activation of inflammatory mediators in brain [15]. The differing genetic backgrounds of the two AD models may play a role in these discrepancies in neuroinflammatory outcomes. The genetic background of Tg2576 mice, unlike 3xTg-AD mice, includes the genetic contribution of SJL, a strain in which autoimmune encephalitis is often modeled (reviewed by [36]). Employing HSV amplicon-based vaccines to elicit antigen specific responses devoid of autoimmune and inflammatory reactivities will require systematic assessment of immune responses achieved through different routes of inoculation, differing genetic backgrounds, co-expression of various immunomodulating factors such as interleukin-4, and design of Aβ pathogenic peptides with varying structural epitope characteristics. Additionally, experiments in predictive mouse models of AD are required to determine the degree to which genetic background and T cell memory responses participate in the safety, protective action and durability of the amplicon-based Aβ vaccines. This more refined approach will not only enable the development of novel AD immunotherapeutics, but will contribute to the mechanistic dissection of AD pathogenesis and the immune responses required to mediate protection.

Materials and Methods

Cell culture

Baby hamster kidney (BHK) cells were maintained as previously described [37]. The NIH-3T3 mouse fibroblast cell line was originally obtained from American Type Culture Collection and maintained in Dulbecco's modified Eagle medium plus 10% fetal bovine serum.

Amplicon construction and helper virus-free amplicon packaging

The $pHSV_{IE}1_{CMV}2$ parental amplicon vector was constructed by removing the CMV immediate-early promoter/multiple cloning site/polyadenylation signal cassette from pBSpA/CMV using *Kpn*I and *Not*I. This segment was blunted and ligated into a *Bcl*I-cut and blunted

pHSV$_{IE}$1 plasmid to create pHSV$_{IE}$1$_{CMV}$2. The sequence encoding human Aβ$_{1-42}$ was PCR-amplified from pHSVAβ [15] using the following primers: A-Beta.2(+) 5′-CCCGTCTAGAACCATGGATGCAGAATTCCGACATGACTCAGG-3′ and A-Beta.2(-) 5′-CGCGGTACCCTACGCTATGACAACACCGCCCACCAT-3′. The resultant PCR product was digested with *Xba*I and *Kpn*I and inserted into an identical digested pHSV$_{IE}$1$_{CMV}$2 plasmid to create pHSV$_{IE}$Aβ$_{CMV}$2. The mouse IL-4 cDNA was removed from pORF-mIL-4 (Invivogen, San Diego, CA) using *Nco*I and *Nhe*I and blunted with T4 DNA polymerase. This fragment was inserted into an *Eco*RV-cut pHSV$_{IE}$Aβ$_{CMV}$2 vector to create pHSV$_{IE}$Aβ$_{CMV}$IL-4. All amplicon vectors were tested for expression by transfection of BHK cells and were packaged using a previously described helper virus-free methodology [23].

3xTg-AD mice

Triple-transgenic Alzheimer's disease (3xTg-AD) mice were created as previously described [21,22]. Eighteen age-matched male 3xTg-AD mice (human PS1^{M146V}, human APP^{SWE}, human tau^{P301L}) were randomized into three treatment groups (N = 6 male mice per group). Six age-matched male 3xTg-AD mice that were not vaccinated (NVC) were sacrificed at 11 months of age to serve as controls in immunohistochemical analyses. All experiments were conducted under protocols approved by the National Institutes of Health and mice were housed in the University of Rochester Medical Center Vivarium, which is fully accredited by the Association for the Assessment and Accreditation of Laboratory Animal Care. After weaning, mice were genotyped using PCR as previously described and were group housed [21,22]. All mice were maintained on a 12-h light: 12-h dark cycle with *ad libitum* access to rodent chow and water.

Vaccination paradigm and serum isolation

Two month-old 3xTg-AD male mice were vaccinated via the subcutaneous (SQ) route with one of the following amplicons: HSV$_{IE}$Aβ$_{CMV}$2, HSV$_{IE}$Aβ$_{CMV}$IL-4, or the no-insert control HSV$_{IE}$1$_{CMV}$2. The vaccination schedule consisted of three separate injections at 2, 3, and 9 months of age. Blood was collected from the lateral tail vein two weeks after each injection. Prior to each blood draw mice were anesthetized with avertin (300 mg/kg). The blood was allowed to clot, then placed at 4°C overnight to facilitate separation of the serum from the clot. The clots were removed and the serum centrifuged at 10,000 × g for 10 min. to pellet any remaining blood cells and debris. The clarified serum was transferred to a fresh tube and stored at -20°C until analyzed by ELISA.

ELISA analyses

Mouse IL-4 levels in amplicon plasmid-transfected cell culture supernatants were determined by use of a mouse IL-4 specific ELISA according to manufacturer's directions (R&D Systems, Minneapolis, MN). Levels of α-Aβ antibody levels in immunized mouse sera were determined as described previously [15]. Endpoint titers were calculated using the statistical method described by Frey et al. [38]. Antibody isotype analyses were performed as described previously [15].

Barnes Maze

The Barnes Maze was used to study spatial learning and memory functioning in immunized mice as previously described [28,39]. AD immunotherapy-mediated alterations of learning/memory behaviors in AD mouse models have been monitored using the Barnes Maze paradigm previously [40-43]. Modifications included the following: (1) a training trial was performed 1 week prior to, instead of on the first day of actual testing; (2) sessions included three trials per day with a 20-min. inter-trial interval, taking place one day per month at 2, 6, and 11 months of age; (3) the total time to complete the maze was limited to 4 min. instead of 5 min.; and (4)

shredded bedding was placed in the goal box. An observer made additional assessments from behind a 2-way mirror. These included the location of the first hole, the quadrant of the first hole, the number of errors made by the mouse prior to locating the goal box, the time duration required to enter the goal box (latency), and the overall strategy to find the goal box. A video camera was mounted above the maze and was connected to a computer imaging software program (Videomex-One, Columbus Inst. Columbus, OH) to record the total distance traveled.

Immunohistochemical analyses

Immunohistochemical (IHC) analyses of AD-related pathologies in 3xTg-AD mice were performed on immunized 11 month-old 3xTg-AD mice and age-matched non-vaccinated control 3xTg-AD mice as previously described [29] using the following antibodies: mouse monoclonal 6E10 antibody (1:1000, Covance Research Products, Berkeley CA), anti-amyloid precursor protein A4, corresponding to the NPXY motif of hAPP, (Clone Y188; AbCam, Cambridge, MA, 1:750), anti-human tau monoclonal antibody HT7 (1:200, Pierce, Rockford, IL), anti-human phospho-tau monoclonal antibody AT180 (1:200, Pierce, Rockford, IL), astrocytes (1:1000, polyclonal anti-GFAP, Dakocytomation, Glostrup, Denmark) and microglia (1:500, rat anti-mouse F4/80, AbD Serotec, Raleigh, NC).

Modifications include the following: Phosphate buffer (PB) was used instead of PBS, 0.4% PB/Triton-X 100 was used in place of 0.1% PBS/Triton-X 100, and the secondary antibody was incubated for 2 h at 22°C. For HT7, AT180, and GFAP detection the protocol was performed as described except the epitope retrieval step was removed. GFAP staining required the secondary antibody, biotinylated rabbit (1:2000, Vector Laboratories, Burlingame, CA). For F4/80 detection quenching included 3% peroxide, the epitope retrieval was omitted, the primary antibody included 3% normal goat serum (NGS) + 3% BSA instead of 1% NGS, and the secondary antibody was biotinylated rat (1:2000, Vector Laboratories, Burlingame, CA).

Quantification of staining intensity

Quantification of positively stained targets was performed as previously described [29]. Images were obtained at 10x magnification in the CA_1 hippocampal and subiculum regions of the brain using an Olympus AX-70 microscope equipped with a motorized stage (Olympus, Melville, NY). The sections corresponding to 1.28 mm to 2.75 mm posterior from Bregma were analyzed. Estimated target numbers were determined for each area using MCID 6.0 Elite Imaging Software (Imaging Research, Inc.). The numbers of sections quantified for each area were as follows: *Area I (Rostral CA1 hippocampus)*: 8-12 (6E10), 8 (AT180), 6-10 (HT7), 6-12 (hAPP); *Area II (Caudal CA1 hippocampus)*: 8-12 (6E10), 12 (AT180), 6-12 (HT7), 6-12 (hAPP); *Area III (Subiculum)*: 8-12 (6E10), 8-12 (AT180), 8-12 (HT7), 8-12 (hAPP); and *Area IV (Entorhinal Cortex)*: 8-12 (6E10), 12-18 (AT180), 14-18 (HT7), 14-20 (hAPP).

Statistical analyses

Data were analyzed by means of Student T-test or analysis of variance (ANOVA), followed by post-hoc comparison using Bonferroni's method in the GraphPad Prism v.4.0 (GraphPad Prism Software, San Diego, CA) data analysis software package. P<0.05 was considered statistically significant.

Supplementary Material

Refer to Web version on PubMed Central for supplementary material.

References

1. Selkoe DJ. Alzheimer's disease is a synaptic failure. Science 2002;298:789–791. [PubMed: 12399581]

2. Braak H, Braak E. Neuropathological stageing of Alzheimer-related changes. Acta Neuropathol (Berl) 1991;82:239–259. [PubMed: 1759558]

3. Braak H, Braak E. Frequency of stages of Alzheimer-related lesions in different age categories. Neurobiol Aging 1997;18:351–357. [PubMed: 9330961]

4. Tariot PN, Federoff HJ. Current treatment for Alzheimer disease and future prospects. Alzheimer Dis Assoc Disord 2003;17(Suppl 4):S105–113. [PubMed: 14512816]

5. Hardy J, Selkoe DJ. The amyloid hypothesis of Alzheimer's disease: progress and problems on the road to therapeutics. Science 2002;297:353–356. [PubMed: 12130773]

6. Janus C, Pearson J, McLaurin J, Mathews PM, Jiang Y, Schmidt SD, et al. A beta peptide immunization reduces behavioural impairment and plaques in a model of Alzheimer's disease. Nature 2000;408:979–982. [PubMed: 11140685]

7. Morgan D, Diamond DM, Gottschall PE, Ugen KE, Dickey C, Hardy J, et al. A beta peptide vaccination prevents memory loss in an animal model of Alzheimer's disease. Nature 2000;408:982–985. [PubMed: 11140686]

8. Schenk D, Barbour R, Dunn W, Gordon G, Grajeda H, Guido T, et al. Immunization with amyloid-beta attenuates Alzheimer-disease-like pathology in the PDAPP mouse. Nature 1999;400:173–177. [PubMed: 10408445]

9. Dodart JC, Bales KR, Gannon KS, Greene SJ, DeMattos RB, Mathis C, et al. Immunization reverses memory deficits without reducing brain Abeta burden in Alzheimer's disease model. Nat Neurosci 2002;5:452–457. [PubMed: 11941374]

10. Kotilinek LA, Bacskai B, Westerman M, Kawarabayashi T, Younkin L, Hyman BT, et al. Reversible memory loss in a mouse transgenic model of Alzheimer's disease. J Neurosci 2002;22:6331–6335. [PubMed: 12151510]

11. Bowers WJ, Federoff HJ. Amyloid immunotherapy-engendered CNS inflammation. Neurobiol Aging 2002;23:675–676. [PubMed: 12392770]discussion 683-674

12. Orgogozo JM, Gilman S, Dartigues JF, Laurent B, Puel M, Kirby LC, et al. Subacute meningoencephalitis in a subset of patients with AD after Abeta42 immunization. Neurology 2003;61:46–54. [PubMed: 12847155]

13. Hock C, Konietzko U, Papassotiropoulos A, Wollmer A, Streffer J, von Rotz RC, et al. Generation of antibodies specific for beta-amyloid by vaccination of patients with Alzheimer disease. Nat Med 2002;8:1270–1275. [PubMed: 12379846]

14. Zhang J, Wu X, Qin C, Qi J, Ma S, Zhang H, et al. A novel recombinant adeno-associated virus vaccine reduces behavioral impairment and beta-amyloid plaques in a mouse model of Alzheimer's disease. Neurobiol Dis 2003;14:365–379. [PubMed: 14678754]

15. Bowers WJ, Mastrangelo MA, Stanley HA, Casey AE, Milo LJ Jr. Federoff HJ. HSV amplicon-mediated Abeta vaccination in Tg2576 mice: differential antigen-specific immune responses. Neurobiol Aging 2005;26:393–407. [PubMed: 15653168]

16. Frenkel, N. Defective interfering herpesviruses. In: Nahmias, A.; Dowdle, W.; Scchinazy, R., editors. The human herpesviruses- an interdisciplinary prospective. Elsevier-North Holland, Inc.; New York: 1981. p. 91-120.

17. Frenkel, N.; Spaete, RR.; Vlazny, DA.; Deiss, LP.; Locker, H. The herpes simplex virus amplicon - a novel animal-virus cloning vector. In: Gluzman, Y., editor. Eucaryotic Viral Vectors. Cold Spring Harbor Laboratory; New York: 1982. p. 205-209.

18. Geller AI, Breakefield XO. A defective HSV-1 vector expresses *Escherichia coli* β-galactosidase in cultured peripheral neurons. Science 1988;241:1667–1669. [PubMed: 2843986]

19. Spaete RR, Frenkel N. The herpes simplex virus amplicon: A new eucaryotic defective-virus cloning-amplifying vector. Cell 1982;30:305–310. [PubMed: 6751560]

20. Finkelman FD, Shea-Donohue T, Goldhill J, Sullivan CA, Morris SC, Madden KB, et al. Cytokine regulation of host defense against parasitic gastrointestinal nematodes: lessons from studies with rodent models. Annu Rev Immunol 1997;15:505–533. [PubMed: 9143698]

21. Oddo S, Caccamo A, Kitazawa M, Tseng BP, LaFerla FM. Amyloid deposition precedes tangle formation in a triple transgenic model of Alzheimer's disease. Neurobiol Aging 2003;24:1063–1070. [PubMed: 14643377]

22. Oddo S, Caccamo A, Shepherd JD, Murphy MP, Golde TE, Kayed R, et al. Triple-transgenic model of Alzheimer's disease with plaques and tangles: intracellular Abeta and synaptic dysfunction. Neuron 2003;39:409–421. [PubMed: 12895417]

23. Bowers WJ, Howard DF, Brooks AI, Halterman MW, Federoff HJ. Expression of vhs and VP16 during HSV-1 helper virus-free amplicon packaging enhances titers. Gene Ther 2001;8:111–120. [PubMed: 11313780]

24. Bowers WJ, Howard DF, Federoff HJ. Discordance between expression and genome transfer titering of HSV amplicon vectors: recommendation for standardized enumeration. Mol Ther 2000;1:294–299. [PubMed: 10933945]

25. Santos K, Simon DA, Conway E, Bowers WJ, Mitra S, Foster TH, et al. Spatial and temporal expression of herpes simplex virus type 1 amplicon-encoded genes: implications for their use as immunization vectors. Hum Gene Ther 2007;18:93–105. [PubMed: 17298238]

26. Manz RA, Hauser AE, Hiepe F, Radbruch A. Maintenance of serum antibody levels. Annu Rev Immunol 2005;23:367–386. [PubMed: 15771575]

27. Sohn JH, So JO, Kim H, Nam EJ, Ha HJ, Kim YH, et al. Reduced serum level of antibodies against amyloid beta peptide is associated with aging in Tg2576 mice. Biochem Biophys Res Commun 2007;361:800–804. [PubMed: 17678618]

28. Barnes CA. Memory deficits associated with senescence: A neurophysiological and behavioral study in the rat. J Comp Physiol Psychol 1979;93:74–104. [PubMed: 221551]

29. Janelsins MC, Mastrangelo MA, Oddo S, LaFerla FM, Federoff HJ, Bowers WJ. Early correlation of microglial activation with enhanced tumor necrosis factor-alpha and monocyte chemoattractant protein-1 expression specifically within the entorhinal cortex of triple transgenic Alzheimer's disease mice. J Neuroinflammation 2005;2:23. [PubMed: 16232318]

30. Nicoll JA, Wilkinson D, Holmes C, Steart P, Markham H, Weller RO. Neuropathology of human Alzheimer disease after immunization with amyloid-beta peptide: a case report. Nat Med 2003;9:448–452. [PubMed: 12640446]

31. O'Toole M, Janszen DB, Slonim DK, Reddy PS, Ellis DK, Legault HM, et al. Risk factors associated with beta-amyloid(1-42) immunotherapy in preimmunization gene expression patterns of blood cells. Arch Neurol 2005;62:1531–1536. [PubMed: 16216935]

32. Ferrer I, Boada Rovira M, Sanchez Guerra ML, Rey MJ, Costa-Jussa F. Neuropathology and pathogenesis of encephalitis following amyloid-beta immunization in Alzheimer's disease. Brain Pathol 2004;14:11–20. [PubMed: 14997933]

33. Hsiao KK, Scott M, Foster D, Groth DF, DeArmond SJ, Prusiner SB. Spontaneous neurodegeneration in transgenic mice with mutant prion protein. Science 1990;250:1587–1590. [PubMed: 1980379]

34. Sigurdsson EM, Knudsen E, Asuni A, Fitzer-Attas C, Sage D, Quartermain D, et al. An attenuated immune response is sufficient to enhance cognition in an Alzheimer's disease mouse model immunized with amyloid-beta derivatives. J Neurosci 2004;24:6277–6282. [PubMed: 15254082]

35. Oddo S, Billings L, Kesslak JP, Cribbs DH, LaFerla FM. Abeta Immunotherapy Leads to Clearance of Early, but Not Late, Hyperphosphorylated Tau Aggregates via the Proteasome. Neuron 2004;43:321–332. [PubMed: 15294141]

36. Dal Canto MC, Melvold RW, Kim BS, Miller SD. Two models of multiple sclerosis: experimental allergic encephalomyelitis (EAE) and Theiler's murine encephalomyelitis virus (TMEV) infection. A pathological and immunological comparison. Microsc Res Tech 1995;32:215–229. [PubMed: 8527856]

37. Lu B, Federoff HJ. Herpes simplex virus type 1 amplicon vectors with glucocorticoid-inducible gene expression. Hum Gene Ther 1995;6:421–430.

38. Frey A, Di Canzio J, Zurakowski D. A statistically defined endpoint titer determination method for immunoassays. J Immunol Methods 1998;221:35–41. [PubMed: 9894896]

39. Bach ME, Hawkins RD, Osman M, Kandel ER, Mayford M. Impairment of spatial but not contextual memory in CaMKII mutant mice with a selective loss of hippocampal LTP in the range of the θ frequency. Cell 1995;81:905–915. [PubMed: 7781067]

40. Harrison FE, Reiserer RS, Tomarken AJ, McDonald MP. Spatial and nonspatial escape strategies in the Barnes maze. Learn Mem 2006;13:809–819. [PubMed: 17101874]

41. Jensen MT, Mottin MD, Cracchiolo JR, Leighty RE, Arendash GW. Lifelong immunization with human beta-amyloid (1-42) protects Alzheimer's transgenic mice against cognitive impairment throughout aging. Neuroscience 2005;130:667–684. [PubMed: 15590151]

42. Pompl PN, Mullan MJ, Bjugstad K, Arendash GW. Adaptation of the circular platform spatial memory task for mice: use in detecting cognitive impairment in the APP(SW) transgenic mouse model for Alzheimer's disease. J Neurosci Methods 1999;87:87–95. [PubMed: 10065997]

43. King DL, Arendash GW, Crawford F, Sterk T, Menendez J, Mullan MJ. Progressive and gender-dependent cognitive impairment in the APP(SW) transgenic mouse model for Alzheimer's disease. Behav Brain Res 1999;103:145–162. [PubMed: 10513583]

a HSV Amplicon Plasmids
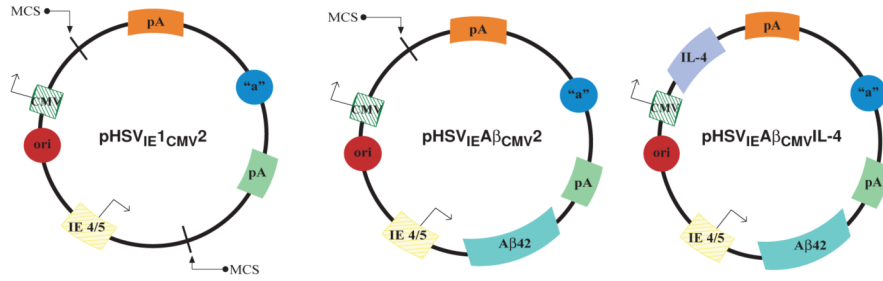
b IL-4 ELISA
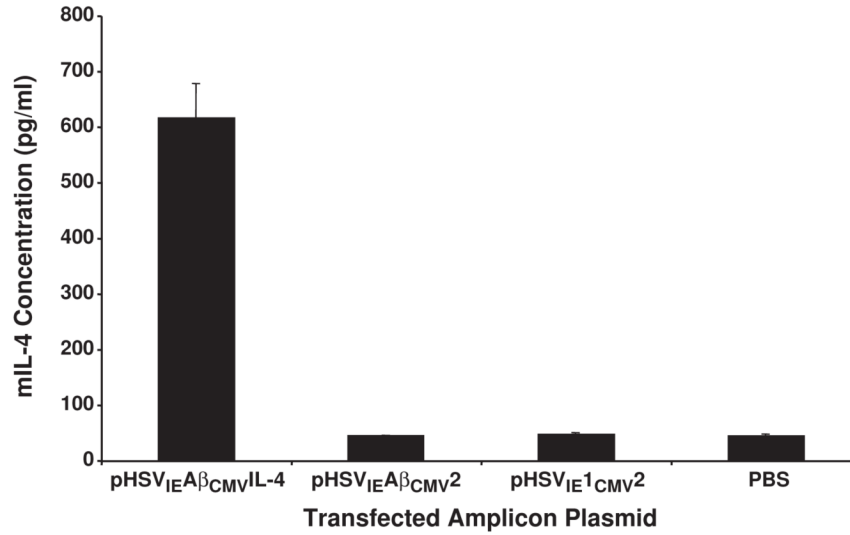
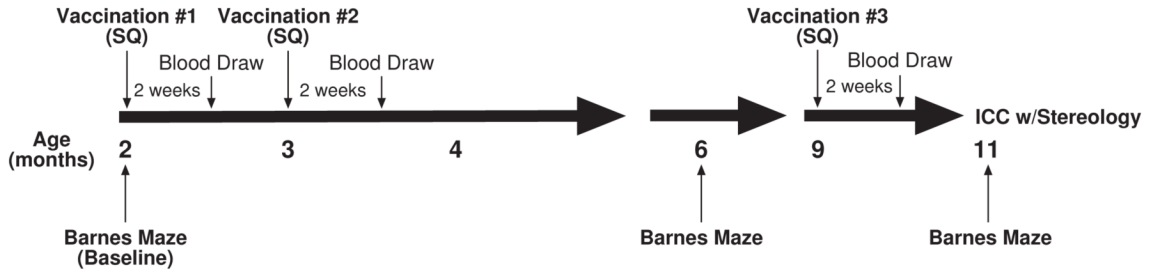
c Experimental Timeline

Figure 1. Schematic representation of newly constructed amplicon vectors, *in vitro* confirmation of amplicon-mediated murine IL-4 expression, and study design

(a) Three kanamycin-resistant HSV amplicons plasmids were constructed: one that served as an empty vector control (pHSV$_{IE}$1$_{CMV}$2) with HSV origin of replication (ori) and HSV packaging signal ("a"), a second (pHSV$_{IE}$Aβ$_{CMV}$2) that expressed the Aβ$_{1-42}$ peptide derived from human amyloid precursor protein (APP) under the transcriptional control of the HSV immediate-early (IE) 4/5 gene promoter and SV40 polyadenylation signal (pA), and a third (pHSV$_{IE}$Aβ$_{CMV}$IL-4) that expressed Aβ$_{1-42}$ via the IE4/5 promoter/SV40 pA transcription unit and murine Interleukin-4 under the separate transcriptional control of the cytomegalovirus (CMV) immediate-early promoter and bovine growth hormone polyadenylation signal. All

amplicons were packaged using a previously described helper virus-free method [23]. **(b)** Each amplicon plasmid was transiently transfected into baby hamster kidney (BHK) cells and culture supernatants were analyzed by ELISA to assess murine IL-4 expression (pg/ml) from the $pHSV_{IE}A\beta_{CMV}IL-4$ amplicon (N=4 per experimental group). A phosphate-buffered saline (PBS) group served as a no-vector control condition. **(c)** A Barnes maze behavioral assessment was performed to determine baseline learning and memory functioning at 2 months of age. Each packaged vector (1×10^6 transduction units) was delivered subcutaneously (SQ) to a randomized cohort of male 3xTg-AD mice [22] (N=6 per experimental group). Amplicons were administered to each animal thrice, and humoral assessments were performed 2 weeks after each vaccination. An intermediate Barnes maze assessment was performed at 6 months of age. Antibody isotype analysis was performed on sera obtained at the 9-month post-initial vaccination time point. Vaccinated mice were sacrificed at 11 months of age at which time endpoint behavioral, histological, and stereological analyses were performed.

a Aβ42-specific ELISA
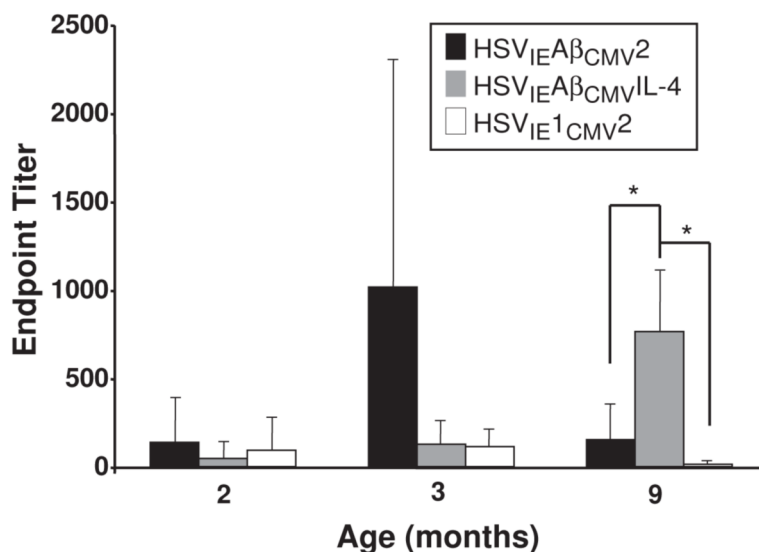
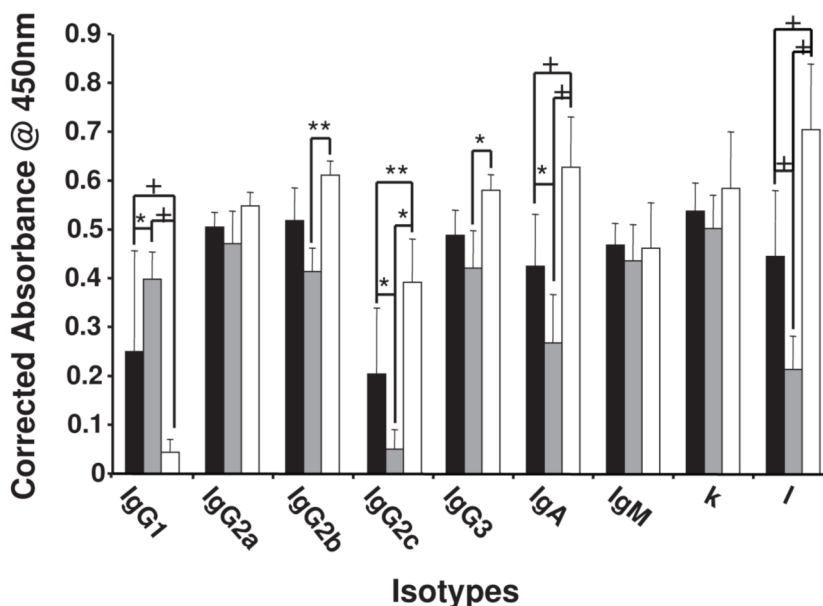**b** Aβ42-specific Isotype ELISA @ 9 months of age

Figure 2. Elicitation of distinctive humoral responses in HSV amplicon vector-vaccinated 3xTg-AD mice

(a) Helper virus-free $HSV_{IE}Aβ_{CMV}2$ (black bars), $HSV_{IE}Aβ_{CMV}IL-4$ (grey bars), and $HSV_{IE}1_{CMV}2$ (open bars) were delivered subcutaneously thrice to 3xTg-AD mice beginning at 2 months of age ($1×10^6$ transduction units per vaccination). Serum was obtained from each vaccinated mouse according to the schema illustrated in Figure 1 and serum samples were analyzed for levels of antibodies binding specifically to the $Aβ_{1-42}$ peptide in quadruplicate by ELISA. Levels of Aβ-specific antibodies arising from each vaccination were corrected using serum isolated from control mice, and are expressed as endpoint titers. (b) Isotypes of α-$Aβ_{1-42}$ antibodies were determined by ELISA using sera obtained at the 9-month time point

from vaccinated 3xTg-AD mice. Levels of Aβ-specific antibody isotypes arising from each vaccination were corrected using serum isolated from control mice, and are expressed as "Corrected Absorbance @ 450 nm". Error bars represent standard deviation. "*" equals $P<0.05$, "**" equals $P<0.01$, and "+" equals $P<0.001$ as determined by two-way ANOVA with Bonferroni post-hoc analysis.
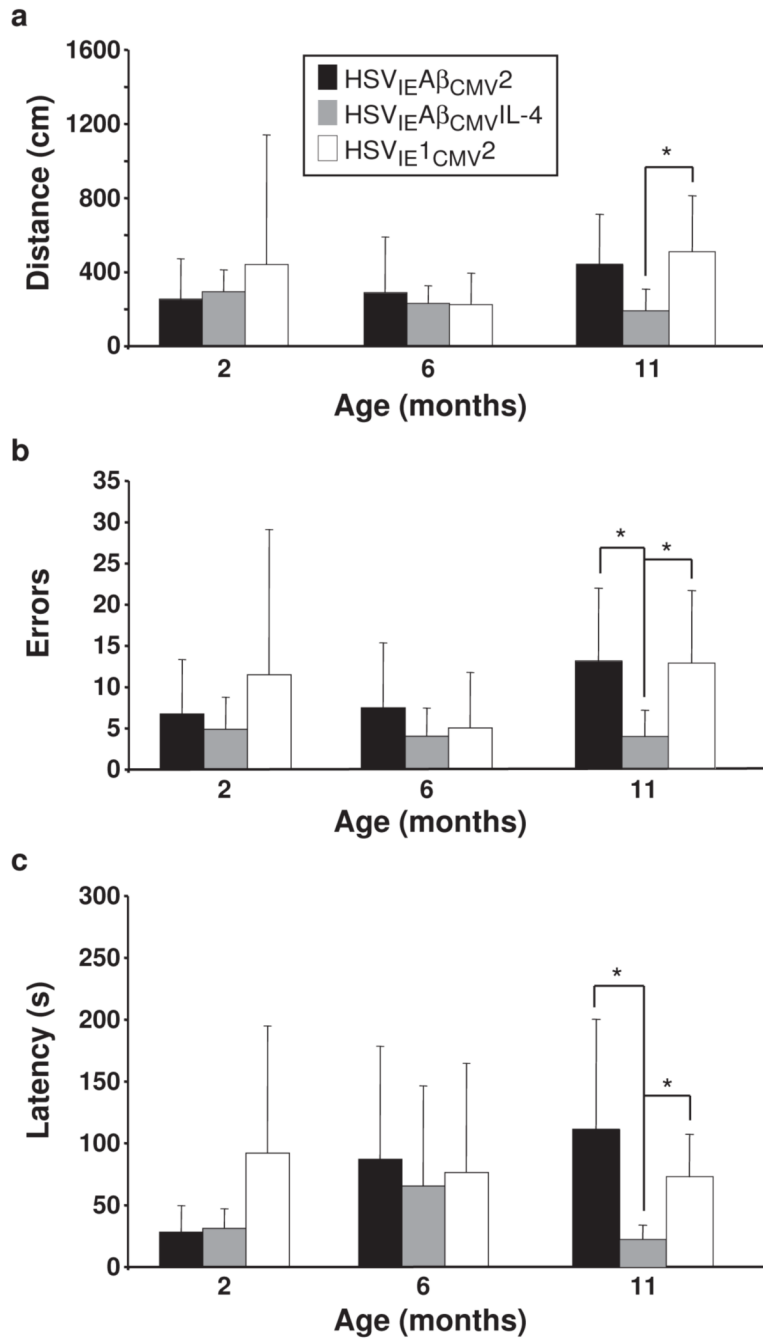
Figure 3. HSV$_{IE}$Aβ$_{CMV}$IL-4 vaccinated 3xTg-AD mice exhibit improved performance in the Barnes maze learning and memory task

Helper virus-free HSV$_{IE}$Aβ$_{CMV}$2 (black bars), HSV$_{IE}$Aβ$_{CMV}$IL-4 (grey bars), and HSV$_{IE}$1$_{CMV}$2 (open bars) were delivered subcutaneously thrice to 3xTg-AD mice beginning at 2 months of age ($1×10^6$ transduction units per vaccination). Mice were tested on the Barnes maze at 2, 6, and 11 months of age to assess the effects of amplicon vaccination on learning/memory functioning using established distance **(a)**, errors **(b)**, and latency **(c)** criteria. Error bars represent standard deviation. "*" equals P<0.05 and "**" equals P<0.01 as determined by one-way ANOVA with Bonferroni post-hoc analysis.
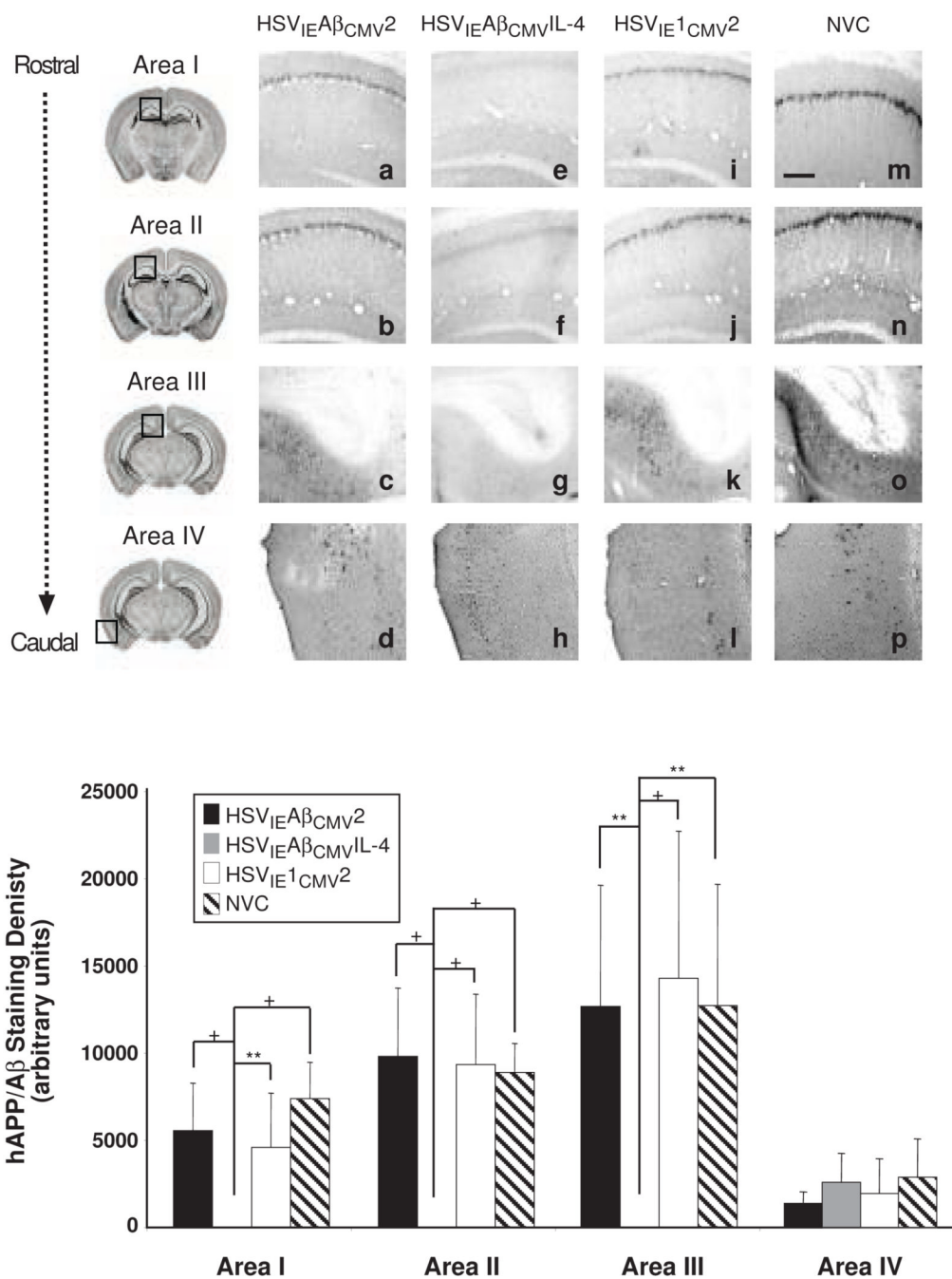
Figure 4. HSV$_{IE}$Aβ$_{CMV}$IL-4 vaccinated 3xTg-AD mice are devoid of amyloid/Aβ burden
Helper virus-free HSV$_{IE}$Aβ$_{CMV}$2 **(a, b, c, d)**, HSV$_{IE}$Aβ$_{CMV}$IL-4 **(e, f, g, h)**, and
HSV$_{IE}$1$_{CMV}$2 **(i, j, k, l)** were delivered subcutaneously thrice to 3xTg-AD mice beginning at
2 months of age (1×10^6 transduction units per vaccination). Coronal mouse brain sections (30
μm) were prepared from vaccinated mice sacrificed at 11 months of age and were processed
for 6E10 immunohistochemistry to assess the extent of human APP/Aβ burden. Age-matched,
non-vaccinated control (NVC) 3xTg-AD mice **(m, n, o, p)** were sacrificed at 11 months of age
and brains processed identically for comparison purposes. Images were obtained for four areas
of the brain. Area I represents the CA$_1$ hippocampal region at -1.28 mm from Bregma **(a, e, i,
m)**, area II represents the CA$_1$ region at -2.12 mm from Bregma **(b, f, j, n)**, area III represents

the subiculum at -2.75 mm from Bregma **(c, g, k, o)**, and area IV represents the entorhinal cortex at -2.50 to -3.80 mm from Bregma **(d, h, l, p)**. The optical densities of immunopositive staining were quantified **(q)**. Black bars represent $HSV_{IE}A\beta_{CMV}2$, grey bars represent $HSV_{IE}A\beta_{CMV}IL$-4, open bars represent $HSV_{IE}1_{CMV}2$, and hatched bars represent non-vaccinated control mice. The scale bar depicted in **m** represents 250 μm. Error bars indicate standard deviation. "*" equals $P<0.05$ and "**" equals $P<0.01$, and "+" equals $P<0.001$ as determined by one-way ANOVA with Bonferroni post-hoc analysis.
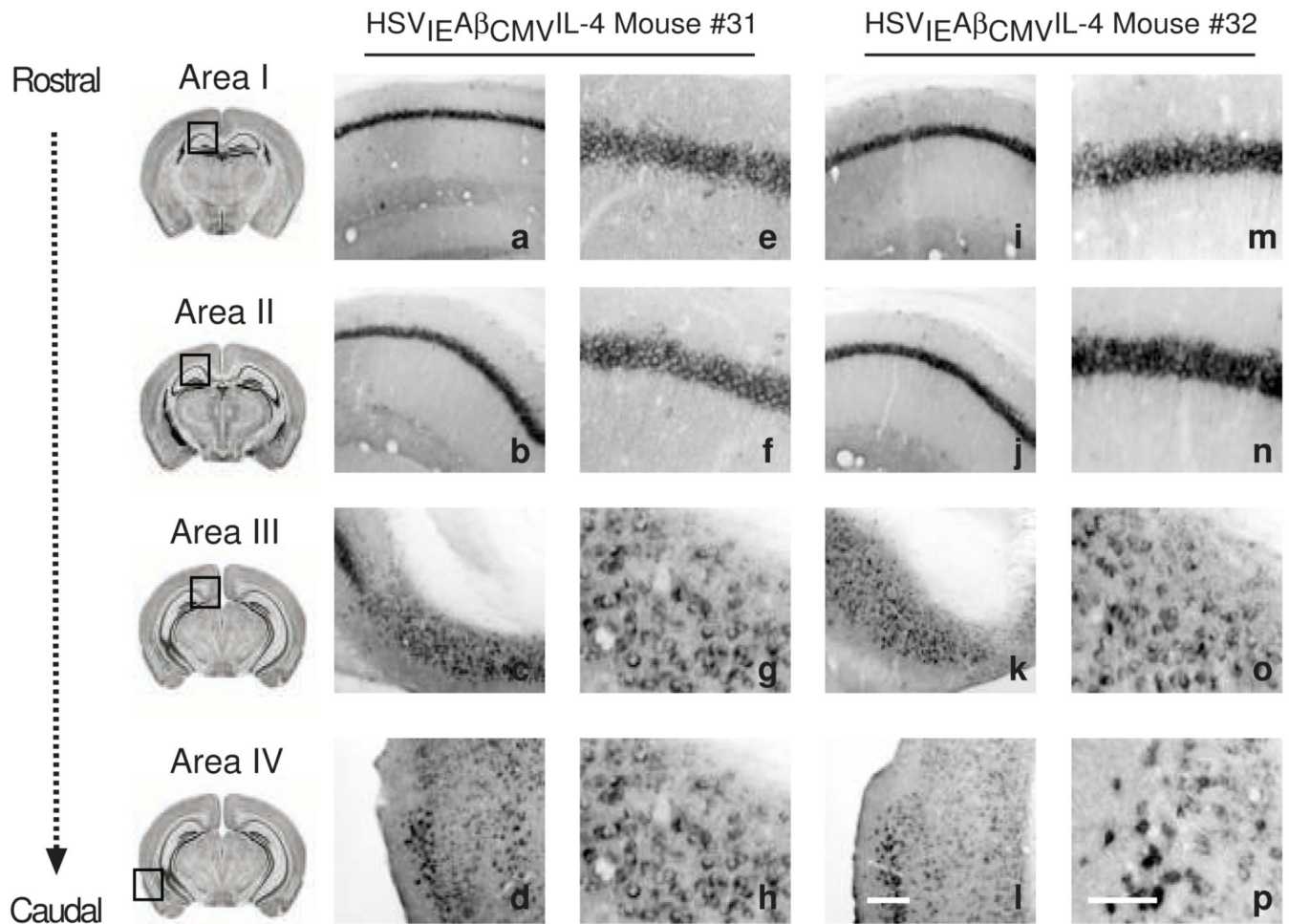
Figure 5. Immunohistochemical analysis of HSV$_{IE}$Aβ$_{CMV}$IL-4 vaccinated 3xTg-AD mice using a human APP-specific antibody demonstrates that vaccination does not affect hAPP^{swe} transgene product levels

A subset of mice vaccinated thrice with helper virus-free HSV$_{IE}$Aβ$_{CMV}$IL-4 **(a-h** and **i-p)** were processed for human APP immunohistochemistry to assess the extent of transgene-derived amyloid precursor protein. Images were obtained for four areas of the brain at low and high magnification shown for two mice (#31 and #32) injected with HSV$_{IE}$Aβ$_{CMV}$IL-4. Area I represents the CA$_1$ hippocampal region at -1.28 mm from Bregma **(a, e, i, m)**, area II represents the CA$_1$ region at -2.12 mm from Bregma **(b, f, j, n)**, area III represents the subiculum at -2.75 mm from Bregma **(c, g, k, o)**, and area IV represents the entorhinal cortex between -2.50 mm and -3.80 mm from Bregma **(d, h, l, p)**. The scale bar depicted in **p** (for panels **e-h** and **m-p**) represents 50 μm. The scale bar depicted in **l** (for panels **a-d** and **i-l**) represents 250 μm.
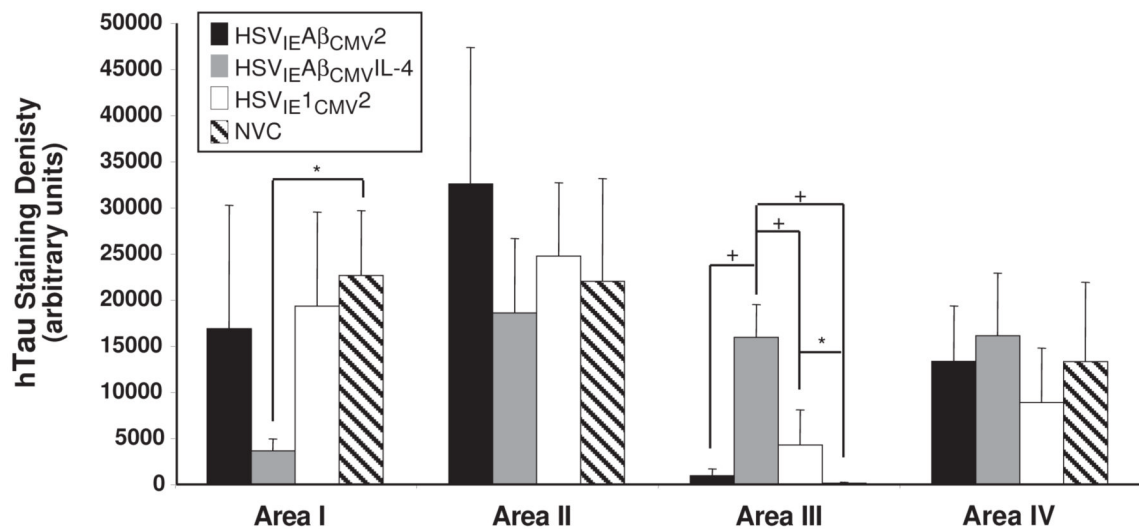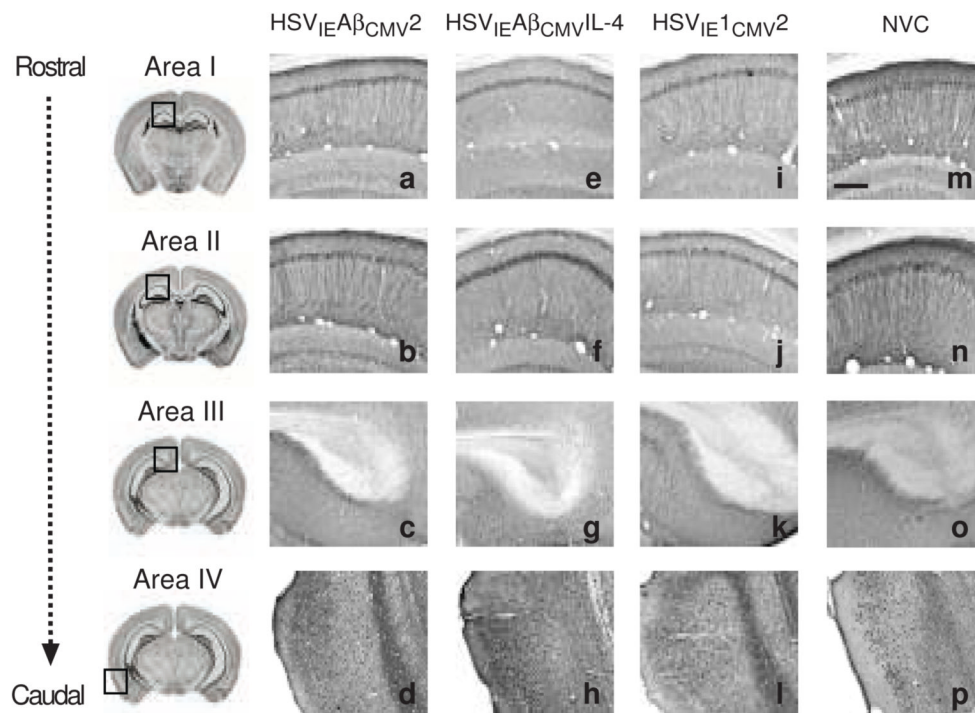
Figure 6. Human tau expression patterns are minimally affected in amplicon-vaccinated 3xTg-AD mice

Helper virus-free HSV$_{IE}$Aβ$_{CMV}$2 **(a, b, c, d)**, HSV$_{IE}$Aβ$_{CMV}$IL-4 **(e, f, g, h)**, and HSV$_{IE}$1$_{CMV}$2 **(i, j, k, l)** were delivered subcutaneously thrice to 3xTg-AD mice beginning at 2 months of age (1×10^6 transduction units per vaccination). Coronal mouse brain sections (30 μm) were prepared from vaccinated mice sacrificed at 11 months of age and were processed for HT7 immunohistochemistry to assess alterations in human Tau transgene expression. Age-matched, non-vaccinated control (NVC) 3xTg-AD mice **(m, n, o, p)** were sacrificed at 11 months of age and brains processed identically for comparison purposes. Images were obtained for four areas of the brain. Area I represents the CA$_1$ hippocampal region at -1.28 mm from

Bregma **(a, e, i, m)**, area II represents the CA_1 region at -2.12 mm from Bregma **(b, f, j, n)**, area III represents the subiculum at -2.75 mm from Bregma **(c, g, k, o)**, and area IV represents the entorhinal cortex at -2.50 to -3.80 mm from Bregma **(d, h, l, p)**. The optical densities of immunopositive staining were quantified **(q)**. Black bars represent $HSV_{IE}A\beta_{CMV}2$, grey bars represent $HSV_{IE}A\beta_{CMV}IL-4$, open bars represent $HSV_{IE}1_{CMV}2$, and hatched bars represent non-vaccinated control mice. The scale bar depicted in **m** represents 250 μm. Error bars indicate standard deviation. "*" equals $P<0.05$ and "+" equals $P<0.001$ as determined by one-way ANOVA with Bonferroni post-hoc analysis.
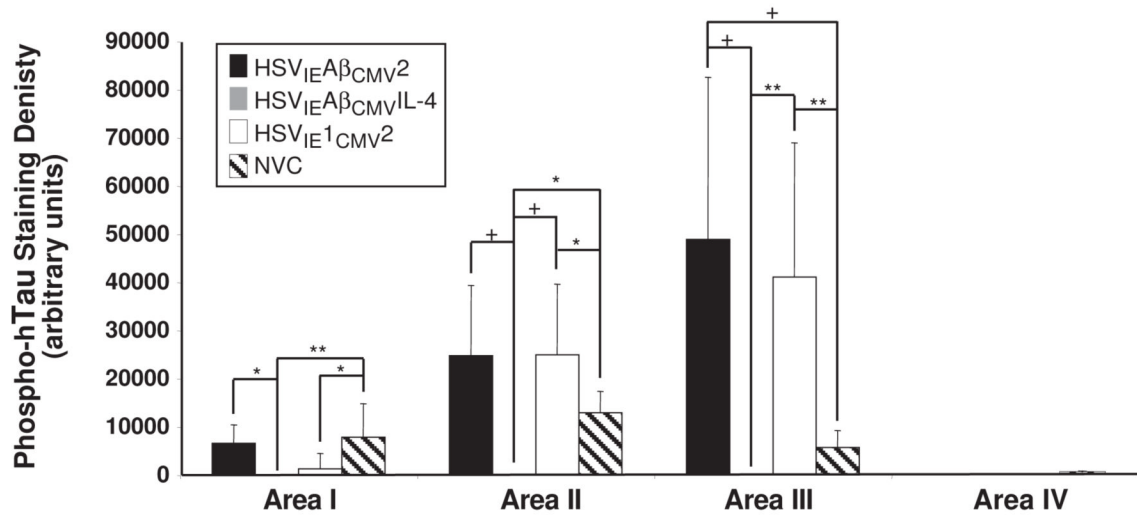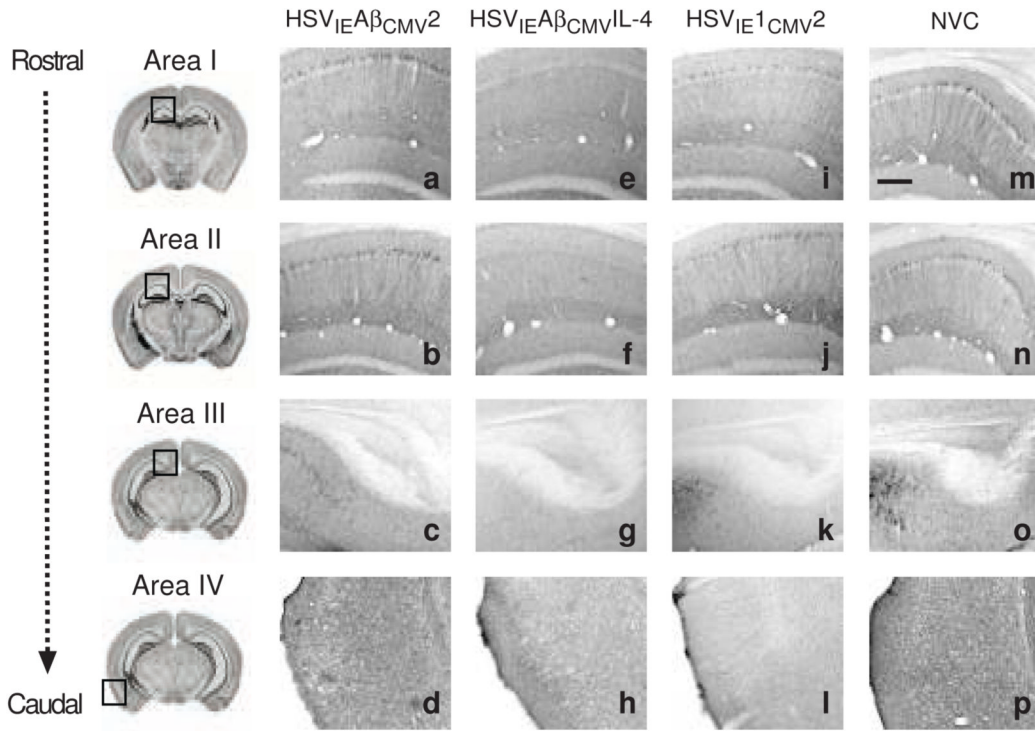
Figure 7. HSV$_{IE}$Aβ_{CMV}IL-4 vaccinated 3xTg-AD mice exhibit suppressed phospho-Tau expression

Helper virus-free HSV$_{IE}$Aβ_{CMV}2 **(a, b, c, d)**, HSV$_{IE}$Aβ_{CMV}IL-4 **(e, f, g, h)**, and HSV$_{IE}$1$_{CMV}$2 **(i, j, k, l)** were delivered subcutaneously thrice to 3xTg-AD mice beginning at 2 months of age (1×10^6 transduction units per vaccination). Coronal mouse brain sections (30 µm) were prepared from vaccinated mice sacrificed at 11 months of age and were processed for AT180 immunohistochemistry to assess alterations in human phospho-Tau pathogenic epitope expression. Age-matched, non-vaccinated control (NVC) 3xTg-AD mice **(m, n, o, p)** were sacrificed at 11 months of age and brains processed identically for comparison purposes. Images were obtained for four areas of the brain. Area I represents the CA$_1$

hippocampal region at -1.28 mm from Bregma **(a, e, i, m)**, area II represents the CA_1 region at -2.12 mm from Bregma **(b, f, j, n)**, area III represents the subiculum at -2.75 mm from Bregma **(c, g, k, o)**, and area IV represents the entorhinal cortex at -2.50 to -3.80 mm from Bregma **(d, h, l, p)**. The optical densities of immunopositive staining were quantified **(q)**. Black bars represent $HSV_{IE}A\beta_{CMV}2$, grey bars represent $HSV_{IE}A\beta_{CMV}IL$-4, open bars represent $HSV_{IE}1_{CMV}2$, and hatched bars represent non-vaccinated control mice. The scale bar depicted in **m** represents 250 μm. Error bars indicate standard deviation. "*" equals $P<0.05$ and "**" equals $P<0.01$, and "+" equals $P<0.001$ as determined by one-way ANOVA with Bonferroni post-hoc analysis.
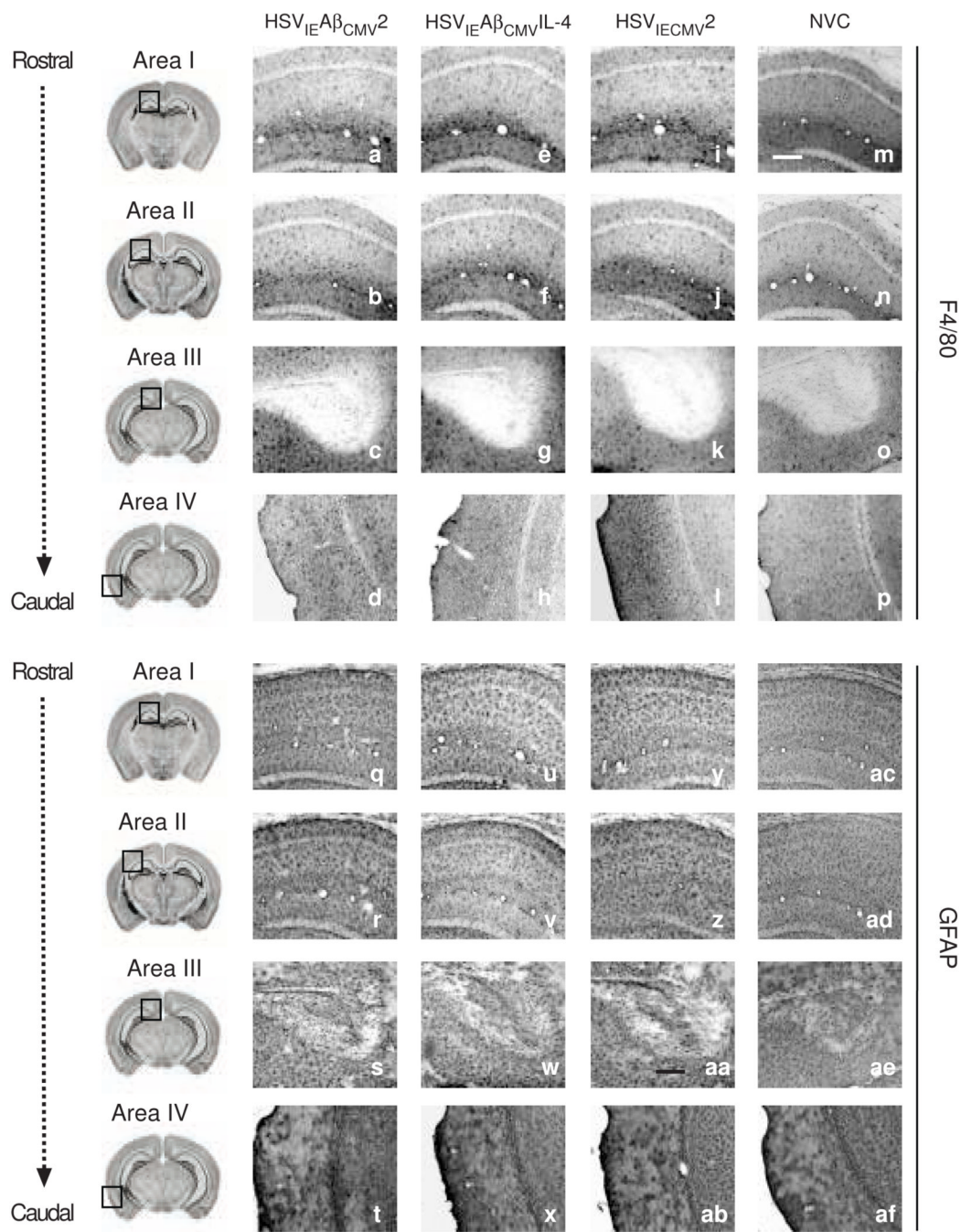
Figure 8. Microglial and astrocytic cell staining patterns in 3xTg-AD mice are not overtly affected by amplicon-mediated vaccination

Helper virus-free HSV$_{IE}$Aβ$_{CMV}$2 **(a-d** and **q-t)**, HSV$_{IE}$Aβ$_{CMV}$IL-4 **(e-h** and **u-x)**, and HSV$_{IE}$1$_{CMV}$2 **(i-l** and **y-ab)** were delivered subcutaneously thrice to 3xTg-AD mice beginning at 2 months of age (1×10^6 transduction units per vaccination). Coronal mouse brain sections (30 μm) were prepared from vaccinated mice sacrificed at 11 months of age and were processed for F4/80 immunohistochemistry **(a-p)** to assess alterations in microglial activation and GFAP immunohistochemistry **(q-af)** to examine changes in astrocyte staining patterns as a result of amplicon-mediated vaccination. Age-matched, non-vaccinated control (NVC) 3xTg-AD mice **(m-p** and **ac-af** for F4/80 and GFAP staining, respectively) were sacrificed at 11 months of

age and brains processed identically for comparison purposes. Images were obtained for four areas of the brain. Area I represents the CA_1 hippocampal region at -1.28 mm from Bregma **(a, e, i, m, q, u, v, ac)**, area II represents the CA_1 region at -2.12 mm from Bregma **(b, f, j, n, r, v, z, ad)**, area III represents the subiculum at -2.75 mm from Bregma **(c, g, k, o, s, w, aa, ae)**, and area IV represents the entorhinal cortex at -2.50 to -3.80 mm from Bregma **(d, h, l, p, t, x, ab, af)**. The scale bar depicted in **m** represents 250 μm.